ELSEVIER

Polymer 42 (2001) 2185–2191

polymer

www.elsevier.nl/locate/polymer

Kinetics for the growth of rigid amorphous fraction in cyclic olefin copolymers (COC)

P.P.-J. Chu[a,*], W.-J. Huang[b], F.-C. Chang[b]

[a]*Department of Chemistry, National Central University, Chung-Li, Taiwan, ROC*
[b]*Institute of Applied Chemistry, National Chaio-Tung University, Hsin-Chu, Taiwan, ROC*

Received 3 February 2000; received in revised form 20 June 2000; accepted 12 July 2000

Abstract

Both linear William–Watts (WW) and non-linear Narayanaswamy–William–Watts (NWW) stretch relaxation satisfactorily described the time dependent rigid amorphous phase growth kinetic. The model is tested upon the completely amorphous cyclic olefin copolymers (COC, polynorbornene/polyethylene copolymer), where a large T_g variation is detected with annealing. Increase of the rigid amorphous fraction as reflected in the increase of T_g, is attributed to the growth of short-range ordered phase due to the rigidity of the norbornene chain segment. The analysis shows the growth kinetic (represented by the retardation time, and the stretch exponent) that depends not only on the norbornene (NB) content but also on the NB microblock structure. The kinetics for the growth of the rigid amorphous domains follows a stretched exponential expression, similar to that given for polymer crystallization and physical aging.

Keywords: Densification; Kinetics; Cyclic olefin copolymers

1. Introduction

In polymers containing rigid monomer segment, self-assembly of the rigid segment upon thermal treatment has lead to the transformation of amorphous phase to more rigid amorphous phase with short-range ordering. Although the rigid amorphous phase does not have a well-defined structure and it does not exhibit as pronounced phase transition as crystallization, this rigid phase bears distinctively different thermal properties from the amorphous phase and it is not entirely disordered. For example, several studies demonstrated the rigid amorphous structure displayed a disordered hexagonal arrangement composed of stiff chains dispersed between the fully ordered crystalline and fully disordered amorphous domain [1]. More pronounced and more rapid changes in free volume and glass temperature with annealing are the few characteristics of samples containing higher fraction of rigid amorphous phase [2–7]. Despite the significant impact of the rigidity in the amorphous phase on polymer physical properties, its kinetics has rarely been studied, however. There are also numerous crystallization studies that indicated solid-state rearrangement into more rigid amorphous phase occurred prior to crystallization [5]. On the basis of entropy, polymers with relatively stiffer chains tend to have higher tendency to form rigid amorphous fraction and thus greater change in glass transition temperature is expected.

Cyclic olefin copolymer (COC) such as polynorbornene/polyethylene copolymer (PNB/PE) is reported to be completely amorphous, and does not crystallize (except in cases when PE content is over 70%) due to its stereoirregularity and regioirregularity [8]. A substantial increase of T_g with annealing is identified and the amorphous to rigid amorphous transformation is confirmed from X-ray diffraction and solid NMR studies. Such phenomenon is not unique to COC. Other amorphous polymers containing rigid monomer unit, such as polycarbonate (PC), poly(phenylene sulfide)(PPS), poly(ethyl ether ketone)(PEEK) and polyimide(PI), also exhibit lower degree of order in the amorphous phase as distorted hexagonal phase diffraction patterns are observed [1]. In the earliest study of PPS, increase in annealing temperature actually results in decrease of T_g [2,3]. On the other hand, PEEK shows no appreciable glass transition change with annealing on the quenched film [4,5]. In spite of clear evidence of the transformation, the kinetics is harder to study due to the relatively small T_g change and the interference from crystallization during the transformation. In addition, the glass transition temperature of the rigid amorphous phase

* Corresponding author. Tel.: +886-3-425-8631; fax: +886-3-422-7664.
E-mail address: pjchu@rs970.ncu.edu.tw (P.P.-J. Chu).

0032-3861/01/$ - see front matter
PII: S0032-3861(00)00586-3

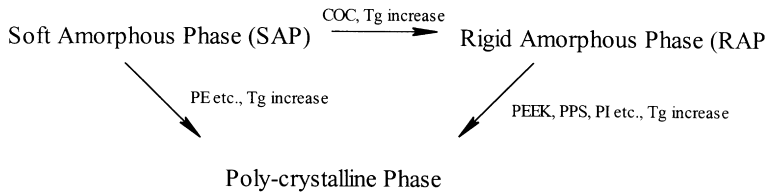

Scheme 1. Structure modifications in polymers and the corresponding T_g variation.

is harder to locate, since it occurs over a broad temperature range with small heat capacity change. The conversion between the two amorphous phases and the crystalline phase in the above-mentioned samples are depicted in Scheme 1.

Purpose of the present study is to examine the kinetics process that underlies the transformation and the driving forces behind these changes. The result is demonstrated using COC as an example, since it is completely amorphous and the T_g variation is huge. As will be seen, the kinetics of the transformation can be followed by a stretch exponential, similar in mathematical form to other non-equilibrium processes in polymer such as physical aging and polymer crystallization.

2. Experimental

COC samples were synthesized by ansa-metallocene catalyst Et(Indenyl)$_2$ZrCl$_2$ and the methyl aluminoxane (MAO) co-catalyst following the procedures described previously [9]. The polymerization temperature was controlled at 66.8°C with a catalyst/co-catalyst ratio of 7000 and the ethylene pressure maintained at 19–21 psi. Ten ml of acidic methanol was used to terminate the activated cation chain end and the COC polymer was precipitated by acetone as the non-solvent. The product was desiccated over 8 h at 50°C under vacuum. Norbornene (NB) block structure of the COC was characterized by high-resolution solution ^{13}C NMR with Bruker DRX-200 where $\nu_H = 200$ MHz. Details of the structure characterization are documented elsewhere [9]. For Run-4, the sample contains the greatest amount of NB block (–N–N– and –N–N–N–) and was not completely dissolvable for reliable solution ^{13}C NMR characterization. Broad line ^{1}H NMR was used to deduce approximate structure characteristics. Calorimetric measurement was obtained from heat flow (ΔC_p) versus temperature (T) with a heating and cooling rate at 10°C/min using Perkin–Elmer DSC-7. Glass transition temperature (T_g) is determined by extrapolating the two straight lines from liquid and glassy states, where the inversion point defined the T_g. Depending upon the transition temperature, the accuracy of T_g varies from 3 to 10°.

Table 1
Microstructure of NB in PNB-*co*-PE by solution ^{13}C NMR (polymerization condition: ethylene pressure = 20 psi, 70°C total volume = 60 ml; [Al]/[Zr] = 8000 ~ 4000; catalyst = 1–2 mg)

Run #	NB content (mol %)	NB microstructure (%)		
		Block	Alternate	Isolate
1	100.0	100	0	0
3	58.4	40.4	51.6	8.0
4	~47.6[a]	>50.0[a]	–	–
5	43.5	17.3	66.6	16.1
6	24.9	21.0	51.0	28.0

[a] Estimated from ^{1}H NMR.

3. Results and discussion

The structural characteristics of the COC samples examined in the study are summarized in Table 1. Fig. 1(a) shows upon annealing the COC ([NB] = 47.63%) at 113°C (15° above the initial T_g), a clear T_g increase with increasing annealing time is found. Although the small heat capacity change during glass transition prevents a clear discretion and the heat capacity diminishes with increases of T_g, the transition temperature can be located from the inflection of the curve using the differential technique indicated by the arrow. A dramatic increase of nearly 50° is apparent.

Shown in Fig. 1(b) are the DSC traces for PNB with annealing time. It is noted that T_g also increases and the final transition temperature after extensive annealing is close to that reported previously with [NB] = 98% [13]. For all samples, T_g is found to increase with annealing time, which are summarized in Fig. 2. As the change in glass temperature reflects directly the free-volume variation under isothermal annealing, the increasing trend of T_g clearly suggested condensation has occurred in these samples. Fig. 3 depicts the initial T_g and that after extended annealing as a function of [NB]. The difference of the two transition temperatures are shown in the insert of Fig. 3 where a clear jump occurs in the composition between 45 and 50 mol% [NB], from about 30 to 75°C. For PNB, the temperature jump is as high as 116°C.

It appears that the degree of densification increases with increasing [NB], but other characteristics are also observed. For samples with relatively low [NB] (<45%), T_g gradually increases with annealing, but for samples having higher [NB] content, a shaper initial rise is also observed (Fig. 2). Previously, CP/MAS studies has demonstrated the unaveraged conformation displays an unusual *gauche* (G) to

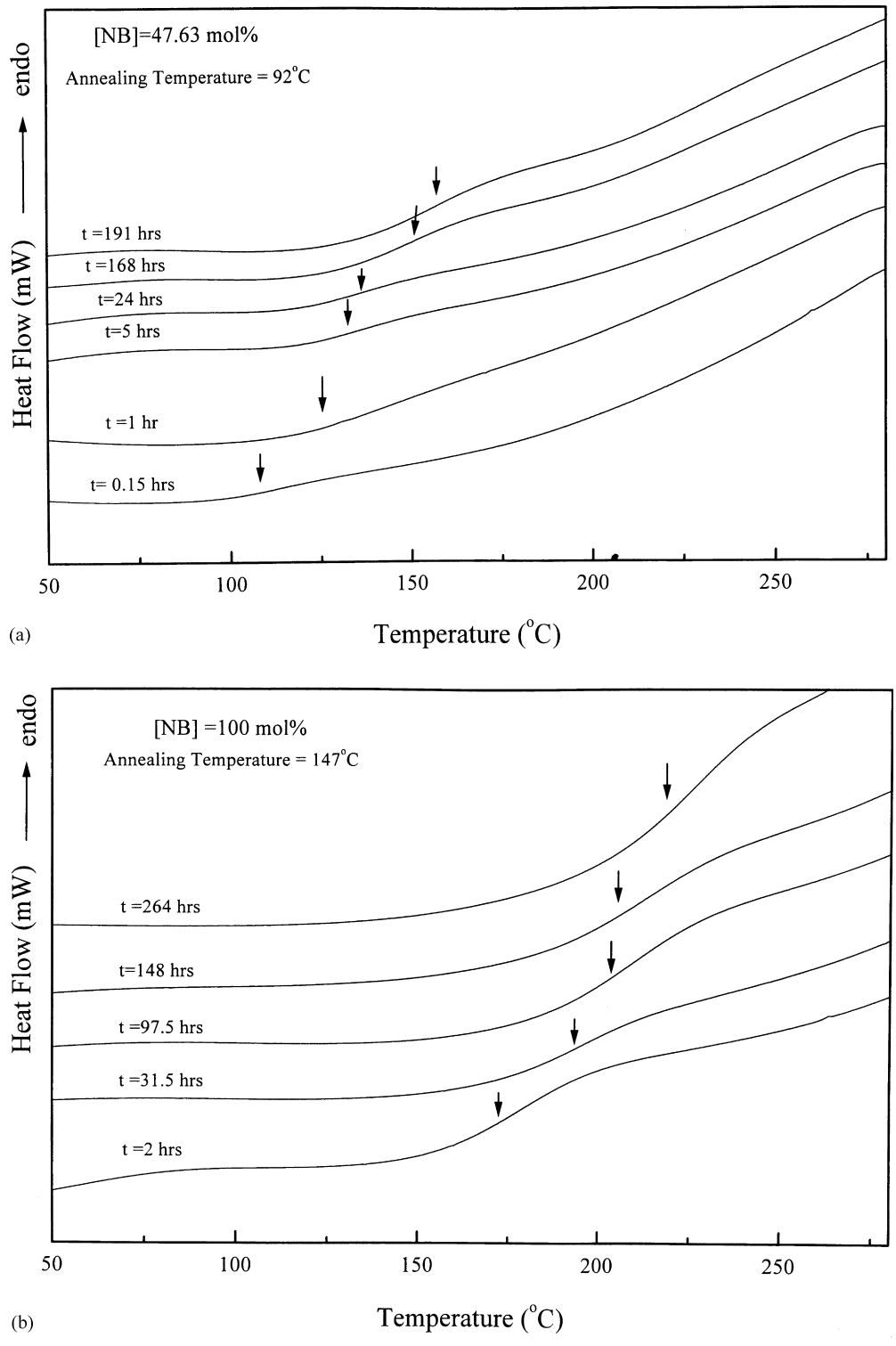

Fig. 1. Changes of glass transition temperature (labeled by arrow) of (a) COC ([NB] = 58.36%) and (b) PNB homopolymer.

trans (T) conformation conversion for COCs with higher amount of continuous NB block. This leads to a more stable T[T]G chain conformation (the bracket in the middle represents the conformation of the NB unit, and the other two to the adjacent single bond) during the initial stage of the annealing. This conversion is responsible for the rapid initial (within the first half hour) increase of T_g for COC's with higher NB content [8].

Regardless of the initial difference, the densification persists for all samples as T_g continue to increase after annealing for 10 h, although the degree of change seem less pronounced in COC with low [NB] where the major

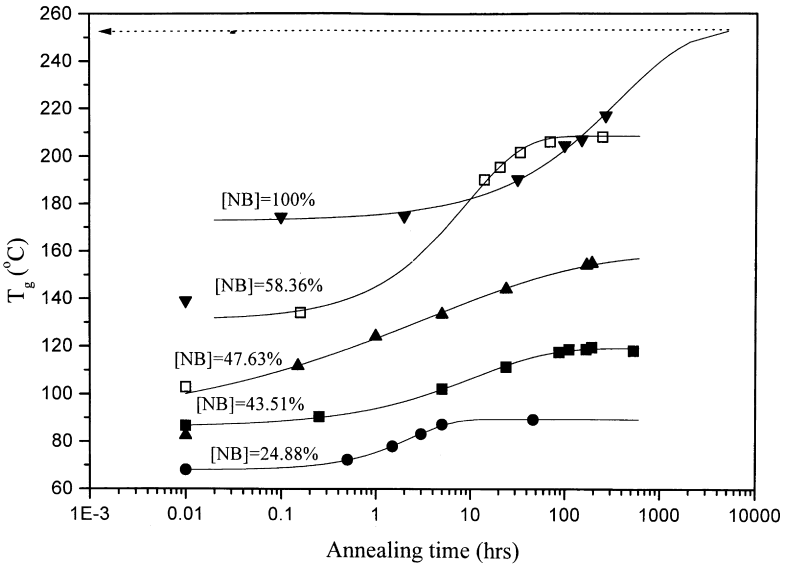

Fig. 2. Variations of T_g increase with annealing time for various COCs. The solid curve is the best fit with the stretched exponential growth model. (See text for details).

structure is composed of isolated and alternating NB units (see Table 2). These results have clearly indicated a densification of the bulk polymer where the rigid chain has rearranged into better short-range ordered structure after extensive annealing. The densification process has been confirmed by synchrotron source X-ray diffraction, where a shift of the averaged long spacing is reduced from 12 to 8.5 Å [14].

The current study is focused on the kinetics of the densification process. This rearrangement process into more rigid amorphous domain is different from the known physical aging behavior where depletion of the free volume is carried out by annealing under the glass temperature. The amorphous to rigid amorphous transformation can be conveniently formulated by considering the volume recovery at arbitrary temperatures. In order to derive the kinetics, the

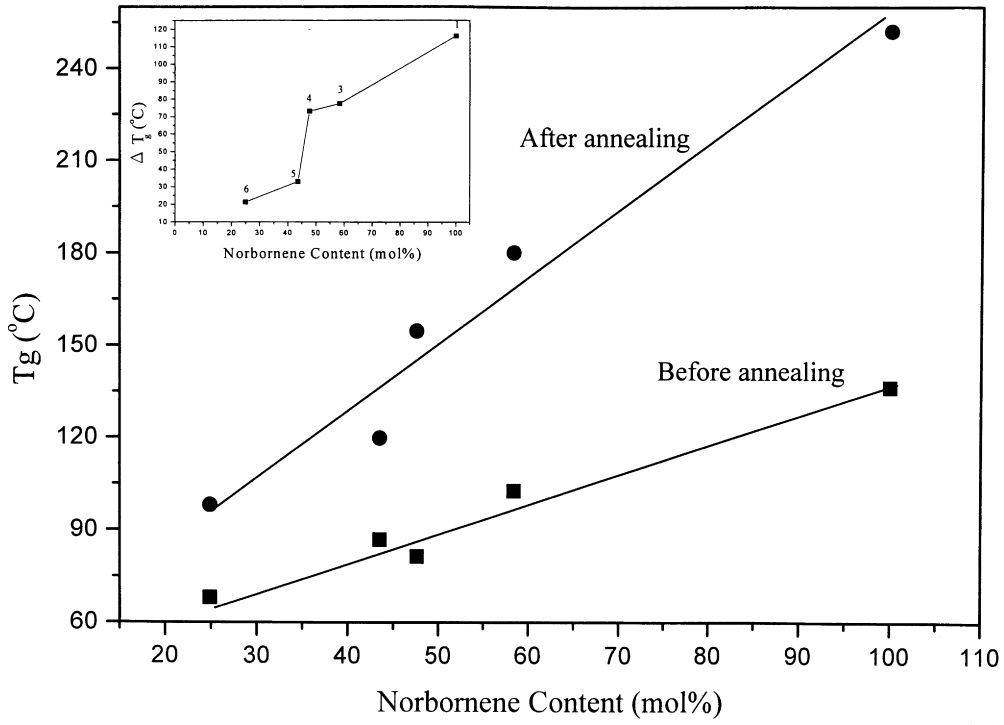

Fig. 3. The initial and final T_gs as a function of the NB content. The inset displays the variation of the size of T_g changes (ΔT_g) as a function of [NB].

Table 2
Results for stretch exponential fitting for T_g variation in COC (the uncertainty in all glass temperature measurements ranges from 3 to 10°)

Run	T_g (i)	T_g (0)[a]	T_g (∞)	ΔT_g[b](°C)	ln(t_d) (h)	$\beta \pm 0.02$
1	136.2	172.7	216.9	44.2	2.56	0.585
3	102.5	130.9	179.9	40.0	0.96	0.73
4	81.3	85.5	154.5	69.0	0.56	0.256
5	86.8	86.1	119.6	33.5	1.05	0.544
6	68.1	68.0	98.0	30.0	0.37	1.0

[a] Obtain from fit to Eq. (7).
[b] $T_g(\infty) - T_g(0)$.

system is conveniently divided into N sub-processes, where the individual glass transition variation in each process is described as:

$$\frac{-\mathrm{d}\delta_i}{\mathrm{d}t} = q\Delta\alpha_i + \frac{\delta_i}{\tau_i} \qquad 1 \le i \le N \tag{1}$$

with

$$\delta_i = T_g - T_g^{\infty} \tag{2}$$

where $\Delta\alpha_i$ is the change of thermal expansion coefficient at T_g in the ith processes, q is the rate of temperature change, τ_i the time constant of the individual sub-process and T_g (∞) the glass temperature of polymer after volume recovery is completed. Assuming that the kinetic is isothermal, and the thermal expansion coefficient α at T_g is unchanged during the course of the densification, the following solution can be reached with suitable boundary condition:

$$\delta_i(t) = \delta_i(0)\left[1 - \exp\left(-\frac{t}{\tau_i}\right)\right] \tag{3}$$

The total relaxation is knowingly the integration over the individual process:

$$\delta(t) = \sum_{i=1}^{N} \delta_i(t) \tag{4}$$

Laplace transformation is employed [11] to arrive an approximate solution of the above integral. This has lead to the stretch exponential with exponent $1 \ge \beta > 0$.

$$\delta(t) = \delta(0)\left[1 - \exp\left(-\frac{t}{t_d}\right)^{\beta}\right] \tag{5}$$

Notice the stretched exponential result reminiscent the linear Williams–Watts (WW) function. However, in a non-linear process, the thermal expansion coefficient is not time independent, and the relaxation is coupled with adjacent processes. The non-linearity is readily formulated following the same treatment of Narayanaswamy by introducing a relaxation time shift factor to the retardation time t_d, i.e. $t_d = t_d^0 t^{\mu}$. [12] The resulting non-linear WW relationship becomes:

$$\delta(t) = \delta(0)\left[1 - \exp\left(-\frac{t}{t_d^N}\right)^{\beta^N}\right] \tag{6}$$

where both$\beta^N = (1-\mu)\beta$ and $t_d^N = (1-\mu)t_d$ are reduced by a factor of $(1-\mu)$ compared to the linear case. Thus, Eq. (6) can be considered as the more general expression for Eq. (5) with $\mu = 0$ representing the linear case.

The stretched relaxation behavior is prevalent in many complex systems of coupled relaxation having totally different random origins. They include glasses, spin-glasses, viscous fluids, disordered dielectrics, and critical binary mixtures [11]. Identification of the process being linear (Eq. (5)) or non-linear (Eq. (6)) is fundamental to accurately interpretate the relaxation parameters. However, since both process are bearing the same mathematical expression, fitting with the experimental results would yield the same parameter sets using either equation. In a complex system, it is impossible to identify the origin and to give independent measurement of the shifting factor μ, except noting its existence. Therefore, the interpretation of the results would be subject to ambiguity regarding the linearity of the process. However, a general understanding and a qualitative comparison of t_d^N and β^N can be made in a series of samples where the shifting factor is not varying substantially, i.e. t_d^N can be taken as the ensemble (time and space) average of the retardation of relaxation in the bulk,

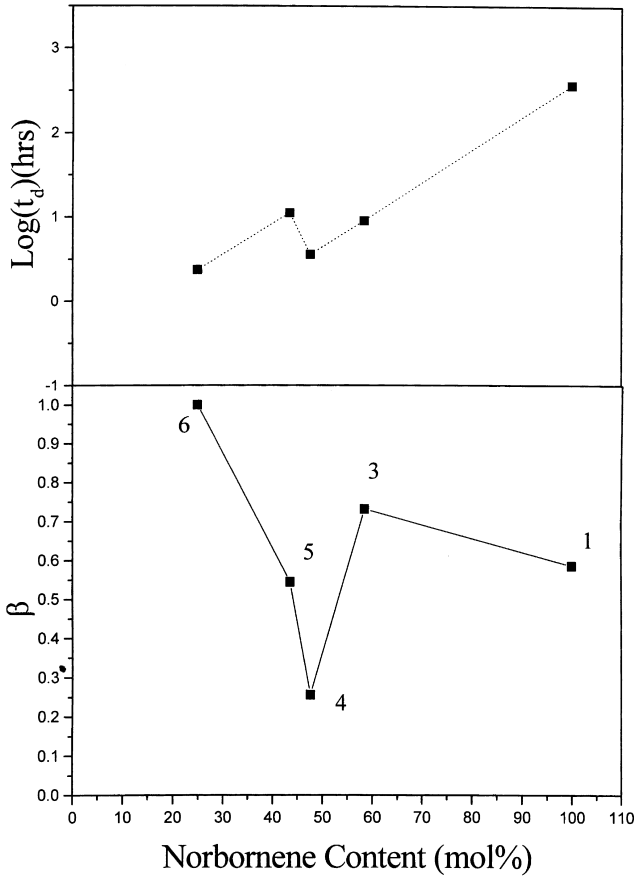

Fig. 4. Variation of t_d^N and stretch exponent β^N with [NB].

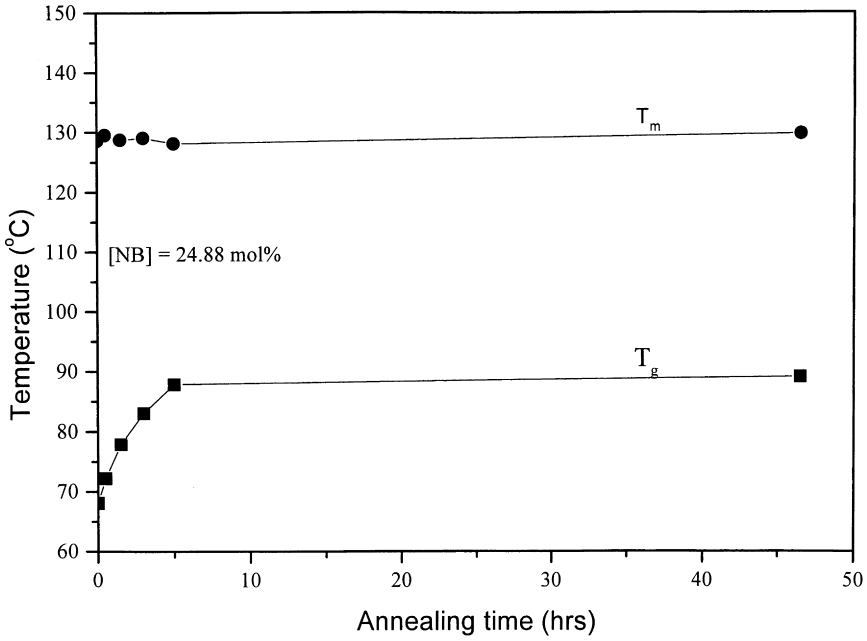

Fig. 5. Variation of both T_m (PE crystalline) and T_g with annealing time. Substantial change in T_g and no apparent change in T_m are observed.

and β^N is used to gauge the dynamic and structural inhomogeneity within the domain [2,3].

The expression for the kinetics of glass temperature variation can be determined, by replacing the corresponding parameters to Eq. (6), which gives:

$$T_g(t) = T_g(0) + \Delta T_g\left[1 - \exp\left(-\frac{t}{t_d^N}\right)^{\beta^N}\right] \quad (7)$$

where T_g is a time-dependent quantity, $\Delta T_g(= T_g(\infty) - T_g(0))$ is the size of the T_g change, with t_d^N the retardation time of the densification process, and β^N the exponent of the stretch exponential. The constant, T_g (0) precedes Eq. (7) is the original glass temperature before annealing, which may be slightly higher than T_g of the as prepared sample as discussed previously. The fitting results (solid curve) based on Eq. (7) are superimposed with the experimental T_g (solid symbols) in Fig. 2 as a function of the logarithm of the annealing time for different COCs. The corresponding kinetic parameters are summarized in the last two columns in Table 2.

The densification retardation time (t_d^N) and the stretch exponent (β^N) are displayed in Fig. 4. It appears that t_d^N increases with [NB] content while β^N is exhibiting a decreasing trend with larger fluctuation. We notice that the rigidity of the chain is governed by the amount of NB block content. Therefore, as the [NB] content increases, the NB microblock unit also increases. In this case, COC is packed more densely in the short-range ordered phase, with longer retardation time t_d^N, and smaller β^N. Since COC is not crystallizable, the densification leads to substantial increase in T_g with annealing.

For COC with PE content greater than 50 mol%, the amorphous phase is composed of disordered PE and non-crystallizable norbornene–ethylene segments. With more frequent interruption of continuous NB block by ethylene, more alternating and isolated NB units appear (Run — 5, 6) which makes the amorphous chain more flexible. This created less entropy difference between the amorphous and short-range ordered phase. As a result, ΔT_g is smaller, and the densification progress with faster rate (shorter t_d^N) with the kinetics approaches simple exponential (β^N close to1.0).

These results suggested that the stiff NB block structure retards transition. However, there are fluctuations for Run-4 and Run-5. The exponent β also shows greatest depression at 0.2 for Run-4 ([NB] = 47.63%). In Fig. 2, we have already noticed that the T_g increase for Run-4 occurs over much longer annealing period. Microstructure analysis (Table 1) indicated this sample contains the highest amount of block NB, even though the NB content is not the highest. Judging from the much smaller t_d^N and β, it is reasonable to assess that the large quantity of the stiff NB block not only retards the transformation, but also leads to more inhomogeneous morphology, or more severely coupled relaxation compared to other COCs. Further characterization is necessary to detail these differences. In any case, the kinetics compels that COC densification is fully contingent upon both the NB content as well as the NB block fine structures.

For COC containing longer PE segment (Run-6 ([NB] = 24.9%), both T_g and T_m (due to long PE segments) are detected and their variations are plotted against annealing time in Fig. 5. This readily implies that PE segment is long enough to exhibit crystallization. Interestingly, while annealing causes substantial increase in T_g, there are only small variations observed for T_m. The absence of crystallite perfection (as T_m do not vary) suggested that PE crystallite

in this COC is rather small and its growth has been severely limited by the rigid NB segment. This small PE crystallite is suspended in the amorphous portion composed mostly of isolated and alternating NB segment. Its contribution to the increase of T_g during the course of the transformation would be quite weak compared to the densification.

Previously, Kovacs–Aklonis–Hutchinson–Ramos (KAHR) model takes into consideration of the "relaxation" and the "memory (or retardation)" nature of the volumetric responses has predicted the experimental measurements obtained at different cooling rates under isothermal recovery below glass temperature [10] We noticed that the processes are similar to the densification illustrated here, but COC densification is carried out above T_g. Although, the derivation for Eqs. (5)–(7) follows entirely different routes as the crystallization and physical aging, it is interesting to note that the kinetics of the conversion follows a stretched exponential form, similar to the Avrami equation.

Current kinetic model can be extended to other systems and to provide deeper insight to the interplay between recrystallization and the densification of the amorphous state. In PPS, increasing annealing temperature actually results in decrease of T_g [2,3]. This may be due to crystallization has reduced the amount of the short-range ordered phase. On the other hand, PEEK, shows no appreciable glass transition change with annealing on the quenched film [4,5]. In this case, the densification may proceed either too rapidly or too slowly for any T_g change to be observable. In comparison with those polymers, the size of T_g variation found in the totally amorphous COC is rather phenomenal.

4. Conclusions

COC shows conversion of amorphous phase to short-range ordered amorphous phase with higher rigidity. A phenomenological stretch exponential relationship is developed to model the kinetics of T_g variation, which reveals the solid-state rearrangement (proceeded by conformational conversion). The re-organization of the rigid chain is similar to crystallization, but in the case of COC, the chain conformation prohibits crystallization, and only the amorphous to short-range ordered amorphous conversion is observed. The substantial changes of T_g (thus growth of ordered amorphous fraction) are found to be function of both NB content and the NB microblock structure. Four unique characteristics in T_g variations are identified with increasing NB content. They are (1) higher initial glass temperature $T_g(i)$, (2) larger T_g deviation, ΔT_g due to greater change in entropy, (3) more pronounced jump from $T_g(0)$ to $T_g(i)$ and (4) longer densification retardation time due to higher chain rigidity. In the case when long NB block present (e.g. Run-4), a more inhomogeneous structure, or more heavily coupled relaxation process is evident as revealed by the much smaller stretch exponent and much shorter retardation time. The study shows that the kinetics for the growth of rigid amorphous phase follows a generalized stretch exponential equation, similar to those observed in crystallization and physical aging.

Acknowledgements

Financial support of this research was provided by the National Science Council of Republic of China under contract no. NSC-87-2113-M-008-004.

References

[1] He C, Griffin; AC, Windle AH. J Appl Polym Sci 1999;72:309.
[2] Lu SX, Cebe P. Polymer 1996;37:4857.
[3] Cheng SZD, Wu ZQ, Wunderlich B. Macromolecules 1987;20:2802.
[4] Elias H-G. Macromolecules. New York: Plenum Press, 1983.
[5] Min J, Benet-Buchholz J, Boese R. Chem Commun 1998:2751.
[6] Peeters M, Goderis B, Reynaers H, Mathot V. J Polym Sci Polym Phys Ed 1999;37:83.
[7] Cantrell GR, McDowell CC, Freeman BD, Noel C. J Polym Sci Polym Phys Ed 1999;37:505.
[8] Chu PP, Huang W-J, Chang F-C. Polymer 1999;41:401.
[9] Chu PP, Teng MS. J Polym Res 2000;7:51.
[10] Wade WG, editor. Polymer physics. New York: Wiley, 1996 (chap. 4).
[11] Degiorgio V, Bellini T, Piazza R. In: Campell IA, Giovannella C, editors. New York: Plenum Press, 1989. p. 155.
[12] Struik LCE. Physical aging in amorphous polymers and other materials. Amsterdam: Elsevier, 1978.
[13] Haselwander TFA, Heitz W, Krugel SA, Wendorff JH. Macromol Chem Phys 1996;197:3435.
[14] Chu PP, Huang W-J, Chang F-C. Macromolecules 2000 (in press).